

Nucleon scattering with higgsino and wino cold dark matter

Brandon Murakami^a and James D. Wells^{a,b}

^(a)*Davis Institute of High Energy Physics*

University of California, Davis, California 95616

^(b)*Lawrence Berkeley National Laboratory, Berkeley, CA 94720*

Abstract

Neutralinos that are mostly wino or higgsino are shown to be compatible with the recent DAMA annual modulation signal. The nucleon scattering rates for these dark matter candidates are typically an order of magnitude above the oft-considered bino. Although thermal evolution of higgsino and wino number densities in the early universe implies that they are not viable dark matter candidates, non-thermal sources, such as from gravitino or moduli decay in anomaly mediated supersymmetry breaking, suggest that they can be the dominant source of cold dark matter. Their stealthiness at high energy colliders gives even more impetus to analyze nucleon scattering detection methods. We also present calculations for their predicted scattering rate with germanium detectors, which have yet to see evidence of WIMP scattering.

hep-ph/0011082

November 2000

1 Introduction

There are two intriguing reasons to study the lightest neutralino from supersymmetric extensions of the Standard Model. For one, we would like an answer for what composes the non-baryonic matter necessary to explain the observed rotations of galaxies. By angular momentum considerations, we note that the observed visible matter in our galaxy implies a lower theoretical angular velocity than observed. We also observe galaxies in clusters insufficiently bound by the visible matter. Secondly, we demonstrate in this article that should light neutralinos exist as a cold dark matter (CDM) candidate, the detection prospects are promising for a wide range of parameter space, including for higgsinos and winos.

In the various supersymmetric models, the sneutrino, the gravitino, and a neutralino are all capable of being the lightest supersymmetric particle (LSP) [1]. Here, we study the lightest neutralino $\tilde{\chi}$ as the LSP. Depending on the supersymmetry breaking model considered, the lightest neutralino may be bino-like, wino-like, higgsino-like, or admixtures of these three categories.

Historically, the bino-like LSP has been studied extensively as a dark matter candidate [2]. The wino-like and higgsino-like LSP have been largely ignored as dark matter candidates because they can be demonstrated in the majority of popular models, that their thermal relic densities are simply too low for dark matter contention [3].

We include the possibility of a relatively new class of models — the anomaly-mediated supersymmetry breaking (AMSB) scenarios [4, 5, 6]. The relevant characteristic of these models is the possibility of a wino-like or higgsino-like LSP (from a non-thermal source) with a density capable of being the dark matter [7, 8]. The wino-like LSP is not unique to the AMSB scenarios. Theoretical grounds are also provided by moduli-dominated supersymmetry breaking within O-II superstring motivated models [9] and supersymmetry breaking in which the responsible F -term is not a $SU(5)$ singlet [10]. What is unique about AMSB is its prediction that the gravitino mass is a few orders of magnitude above the superpartner masses. This characteristic is what ultimately enables the wino or higgsino to be a viable dark matter candidate.

If the lightest neutralino truly is the dark matter or a significant fraction, they, being weakly interacting in character, will penetrate the earth much like a neutrino. This allows for possible detection by scattering elastically with nucleons. Of the different neutralino LSP detection methods [11], we report on the detection prospects of the lightest neutralino scattering off nucleons within different target samples.

2 Supersymmetry Breaking Models

First, a brief review of how the neutralino obtains its character is supplied. The Standard Model includes an electrically neutral U(1) gauge field B and a neutral SU(2) gauge field W^3 . The minimal supersymmetric extension includes two neutral Higgs scalar fields, H_d^0 and H_u^0 . These four fields have supersymmetric fermionic partners $\tilde{\psi} = (\tilde{B}, \tilde{W}^3, \tilde{H}_d^0, \tilde{H}_u^0)$ with various interactions amongst one another, allowing for a non-diagonal mass matrix to be formed out of the Lagrangian quadratic terms. A transformation may be performed to diagonalize the neutralino mass matrix to the physical basis, $\tilde{\chi} = (\tilde{\chi}_1, \tilde{\chi}_2, \tilde{\chi}_3, \tilde{\chi}_4)$, with $\tilde{\chi}_1$ having the smallest mass eigenvalue. The Haber and Kane convention [12] for μ is used in the mass matrix. The notation $\tilde{\chi}$ will be used to mean the lightest neutralino ($\tilde{\chi}_1$). If, for example, the largest component of $\tilde{\chi}$ is the \tilde{W}^3 component, we say the LSP is wino-like. Thus, the LSP's eigenvector components determine its character, as made explicit by

$$\tilde{\chi} = N_{11}\tilde{B} + N_{12}\tilde{W}^3 + N_{13}\tilde{H}_d + N_{14}\tilde{H}_u. \quad (1)$$

We consider gravity mediated and anomaly mediated supersymmetry breaking. The values of M_1 and M_2 are determined within these models, with μ constrained only by additional assumptions on the superpartner spectrum. In a large class of minimal supergravity supersymmetry breaking scenarios, scalar masses m_0 and gauginos M_i are chosen to be the same at the unification scale. In these models, the relation between the U(1) and SU(2) gaugino masses is

$$\frac{M_1}{g_1^2} = \frac{M_2}{g_2^2} \quad (m_{1/2} \text{ universal at GUT scale}). \quad (2)$$

This amounts to $M_1 = \frac{5}{3} \tan^2 \theta_W M_2$ being about half M_2 at the electroweak scale. Within these models, there is still a chance that μ is smaller than M_1 . The lightest neutralino $\tilde{\chi}$ will then be either bino- or higgsino-like for these models.

A wino-like $\tilde{\chi}$ is possible within the AMSB class of models. AMSB models supply two results relevant to our discussion. The first of which claims that the gaugino masses are proportional to the gauge coupling beta function,

$$M_n = \frac{\beta_{g_n}}{g_n} m_{3/2} \quad (\text{AMSB}) \quad (3)$$

where g_n is the gauge coupling constant, $m_{3/2}$ is the gravitino mass, and β_{g_n} is the beta function of the gauge coupling constant. At the electroweak scale, the values of g_n and β_{g_n}

result in M_2 being approximately a third of M_1 . Furthermore, $\mu < M_2$ is possible, depending on the sparticle spectrum. In this case, AMSB would produce a higgsino LSP.

The wino’s cross-section for pair annihilation is higher than the bino’s for two reasons: g_2 is larger than g_1 , and bino pair annihilation has less options for the final state than winos. For example, winos can annihilate to W pairs without any intermediate scalar superpartners whereas pure binos cannot. This results in a present day number density $n_{\tilde{\chi}}$ too low for winos as a cold dark matter candidate (but often just right for binos, which originates its appeal as a cold dark matter candidate). This rules out a wino-like LSP and is the reason the wino-like LSP has been largely ignored as a CDM candidate. Let us call this a “thermal source” for wino production. This discussion also applies to an AMSB-produced higgsino-like LSP.

AMSB supplies a second, “non-thermal source” for $\tilde{\chi}$ production. The gravitino or moduli fields in this model are what constitute the second LSP source via direct or indirect $\tilde{\chi}$ decay products. A modulus field may be defined as the scalar field that parameterizes a flat direction in the theory. The moduli fields may acquire a mass from supersymmetry breaking as the moduli’s own potentials are “lifted” at the ends. The important feature of AMSB models is the granting of a large mass (10 to 100 TeV) to the gravitino and moduli fields. These large masses can circumvent the historically annoying gravitino problem and “cosmological moduli problem” in which the gravitino and moduli acquire small masses under common supergravity models. A small enough mass may have a lifetime longer than successful Big Bang nucleosynthesis would allow. In general, it is undesirable for any cosmological scenario to include a field dumping Planck scale energy into the universe after nucleosynthesis begins. The large masses from AMSB models ensures the gravitino and moduli decay sufficiently early [7, 8].

3 The Scattering Rate

The detection prospects of a neutralino from the galactic halo is quantified as the elastic scattering (or event) rate R . The assumed virialized neutralinos are bound to the galactic halo by a gravitational potential, and the scattering rate (measured in events/day/kg) is [13]

$$R = \frac{\sigma \rho_{\tilde{\chi}} v_{\tilde{\chi}} F_{\xi}}{m_{\tilde{\chi}} M_N}. \quad (4)$$

where $\rho_{\tilde{\chi}} = m_{\tilde{\chi}} n_{\tilde{\chi}}$ is the mass density of the neutralinos, $v_{\tilde{\chi}}$ is the average speed of the neutralinos as they float around the galactic halo, M_N is the mass of the target nucleus, and

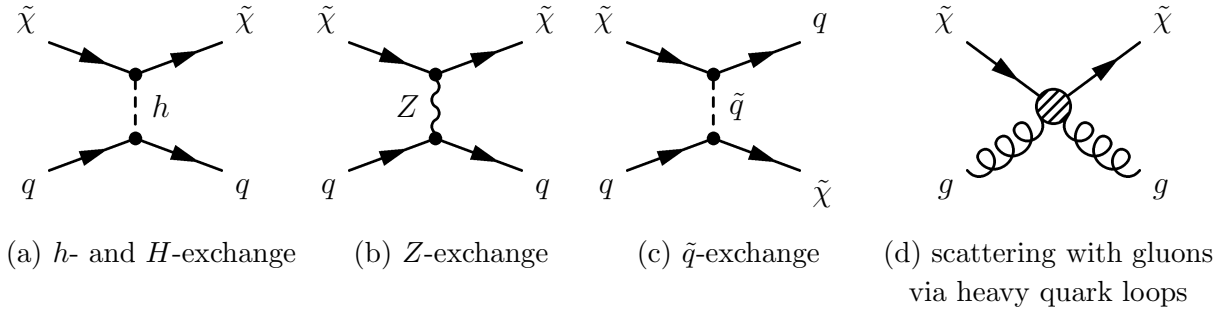


Figure 1: The leading order parton diagrams for $N - \tilde{\chi}$ scattering.

F_ξ is the nuclear form factor (we take $F_\xi = 1$). In terms of the assumed average values, the neutralino's speed and density, the scattering rate is

$$R = \frac{\sigma F_\xi}{m_{\tilde{\chi}} M_N} 1.8 \times 10^{11} \text{GeV}^4 \left(\frac{\rho_{\tilde{\chi}}}{0.3 \text{GeV}/\text{cm}^3} \right) \left(\frac{v_{\tilde{\chi}}}{320 \text{km}/\text{sec}} \right) \left(\frac{\text{events}}{\text{day} \cdot \text{kg}} \right). \quad (5)$$

The scattering cross-section σ is necessary for the scattering rate R , which in turn needs our model's Lagrangian to be made explicit. The Lagrangian is divided into two parts: spin-dependent terms and spin-independent terms. This separation is motivated by realizing spin-independent interactions are enhanced by the presence of all the nucleons in the nucleus.

To describe the spin-independent interactions, we use an effective Lagrangian interaction term of the form

$$\mathcal{L} \subset \sum_{N \in \{p, n\}} f_N [\bar{\tilde{\chi}} \tilde{\chi}] [\bar{N} N], \quad (6)$$

where the subscript N is the nucleon field, proton or neutron. f_N is the scalar 4-point effective coupling constant that includes Higgs and squark exchange, as well as the neutralino-gluon scattering of Fig. 1(d). The contribution of scattering with gluons occurs through a loop of quarks or squarks and is fully calculated in Ref. [14]. It is shown to be at least an order of magnitude smaller than Higgs exchange in Ref. [13] for most of parameter space involving reasonably heavy squarks. For this reason, only one neutralino-gluon interaction is large enough for our task — Higgs exchange to a triangle of heavy quarks (c, b, t) coupled to gluons. These interactions are in addition to another effective Lagrangian term that describes spin-dependent Z , Higgs, and squark exchange:

$$\mathcal{L} \subset [\bar{\tilde{\chi}} \gamma^\mu \gamma^5 \tilde{\chi}] [\bar{q} \gamma_\mu (c_q + d_q \gamma^5) q] \quad (7)$$

where c_q and d_q are effective coupling constants to be made explicit shortly.

These Lagrangian terms yield a scattering cross-section of [13]

$$\sigma = \frac{4}{\pi} \left(\frac{m_{\tilde{\chi}} M_N}{m_{\tilde{\chi}} + M_N} \right)^2 \left[(n_p f_p + n_n f_n)^2 + 4\lambda^2 J(J+1) \left(\sum_{q \in \{u,d,s\}} d_q \Delta q \right)^2 \right]. \quad (8)$$

The factor $\lambda^2 J(J+1)$ represents the fraction of the nucleons' spin in comparison to the total nucleus spin (squared) $J(J+1)$, which includes orbital angular momentum. $m_{\tilde{\chi}}$, n_p , and n_n are the masses of the lightest neutralino, a proton, and a neutron, respectively. Δq is a quark's second moment of the quark density of its spin polarization [15].

The spin-independent effective coupling constant f_N is composed of two terms:

$$f_N = f_H + f_D. \quad (9)$$

The spin-independent squark exchange contributions are organized into terms proportional to the sums and differences of MSSM Yukawa coupling constants $a_{\tilde{q}_i}$ and $b_{\tilde{q}_i}$ from the $\tilde{q}_i q \tilde{\chi}$ vertex, supplied in the Appendix. The terms proportional to $a_{\tilde{q}_i} - b_{\tilde{q}_i}$ are represented by f_D . Those proportional to $a_{\tilde{q}_i} + b_{\tilde{q}_i}$ are small and omitted [13]. f_H is the spin-independent contribution due to Higgs exchange to all six flavors of quarks. The form of f_H is

$$f_H = \sum_{q \in \{u,d,s\}} \frac{f_q^H}{m_q} f_{Tq} m_N + \frac{2}{27} \sum_{q \in \{c,b,t\}} \frac{f_q^H}{m_q} f_{Tg} m_N \quad (10)$$

where f_{Tq} is the fraction of the nucleon mass the light quarks (u, d, s) effectively represent, defined by $f_{Tq} m_N \equiv \langle N | m_q \bar{q} q | N \rangle$ for nucleon N . $f_{Tg} \equiv 1 - \sum f_{Tq}$ is the remaining fraction carried by the nucleon sea. f_q^H is the effective coupling constant for a $f_q^H [\tilde{\chi} \tilde{\chi}] [\bar{q} q]$ Lagrangian term that describes Higgs exchange. f_q^H follows from a straightforward MSSM calculation of h and H t -channel exchange between $\tilde{\chi}$ and a quark:

$$f_q^H = m_q \left(\frac{c_{h\tilde{\chi}\tilde{\chi}} c_{hqq}}{m_h^2} + \frac{c_{H\tilde{\chi}\tilde{\chi}} c_{Hqq}}{m_H^2} \right) \quad (11)$$

where the MSSM Yukawa coupling constants for Higgs-neutralino and Higgs-quark are supplied in the Appendix.

The squark exchange interactions proportional to $a_{\tilde{q}_i}^2 - b_{\tilde{q}_i}^2$ have an effective coupling of

$$f_D = \sum_{q \in \{u,d,s\}} \frac{f_q^{\tilde{q}}}{m_q} f_{Tq} m_N. \quad (12)$$

This refers to simple s -, t -, and u -channel exchanges with the light quarks. All squark exchange interactions proportional to $a_{\tilde{q}_i}^2 - b_{\tilde{q}_i}^2$, denoted f_S , are at least an order of magnitude smaller than the total interaction f , even for reasonably light squarks.

Squark exchange appears as both spin-dependent and spin-independent. The 4-point Lagrangian interaction term implied by s -, t -, and u -channel diagrams of neutralino-quark scattering by squark exchange is $[\bar{q}\tilde{\chi}][\tilde{\chi}q]$. The Fierz rearrangement supplies the scalar form

$$\mathcal{L} \subset f_q^{\tilde{q}} [\tilde{\chi}\tilde{\chi}][\bar{q}q] \quad (13)$$

as well as the vector/axial-vector form

$$\mathcal{L} \subset [\tilde{\chi}\gamma^\mu\gamma^5\tilde{\chi}][\bar{q}\gamma_\mu(c_q^{\tilde{q}} + d_q^{\tilde{q}}\gamma^5)q], \quad (14)$$

where $f_q^{\tilde{q}}$, $c_q^{\tilde{q}}$, and $d_q^{\tilde{q}}$ are effective coupling constants:

$$f_q^{\tilde{q}} = -\frac{1}{4} \sum_{i=1}^2 \frac{a_{\tilde{q}_i}^2 - b_{\tilde{q}_i}^2}{m_{\tilde{q}_i}^2 - (m_{\tilde{\chi}} + m_q)^2} \quad (15)$$

$$c_q^{\tilde{q}} = -\frac{1}{2} \sum_{i=1}^2 \frac{a_{\tilde{q}_i} b_{\tilde{q}_i}}{m_{\tilde{q}_i}^2 - (m_{\tilde{\chi}} + m_q)^2} \quad (16)$$

$$d_q^{\tilde{q}} = \frac{1}{4} \sum_{i=1}^2 \frac{a_{\tilde{q}_i}^2 + b_{\tilde{q}_i}^2}{m_{\tilde{q}_i}^2 - (m_{\tilde{\chi}} + m_q)^2}. \quad (17)$$

$a_{\tilde{q}_i}$ and $b_{\tilde{q}_i}$ refer to the MSSM couplings for the $\tilde{q}q\tilde{\chi}$ vertices and are supplied in the Appendix.

As for spin-dependent interactions, Z -exchange and squark-exchange involve a vector coupling constant c_q and an axial vector coupling constant d_q :

$$c_q = c_q^{\tilde{q}} + c_q^Z, \quad d_q = d_q^{\tilde{q}} + d_q^Z. \quad (18)$$

c_q^Z and d_q^Z are effective coupling constants for a 4-point $\tilde{\chi}\tilde{\chi}qq$ vertex that implicitly proceeds through Z -exchange:

$$c_q^Z = \frac{g_2^2 O_R'' (T_{q3} - 2e_q \sin^2 \theta_W)}{4m_W^2}, \quad d_q^Z = -\frac{g_2^2 O_R'' T_{q3}}{4m_W^2} \quad (19)$$

where T_{q3} is the quark's weak isospin third component, e_q is the electric charge of the quark, and O_R'' is the $Z\tilde{\chi}\tilde{\chi}$ vertex coupling from the MSSM (see the Appendix).

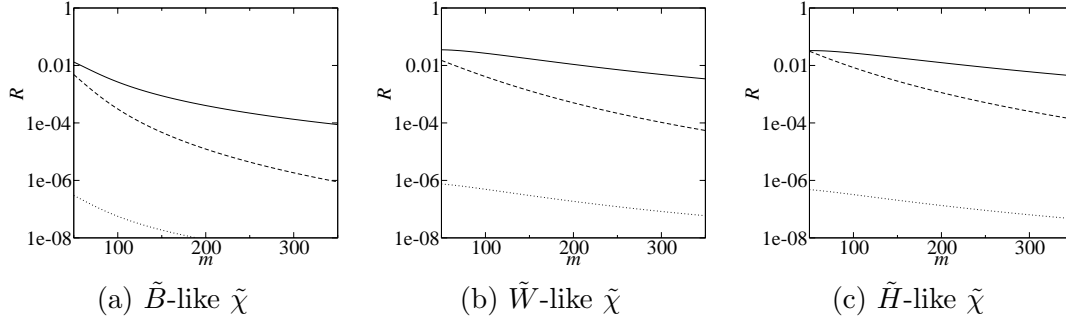


Figure 2: Contributions to R (events/day/kg) vs. $m_{\tilde{\chi}}$ (GeV). These are the contributions to the $\tilde{\chi}$ - ^{73}Ge scattering rate R by Higgs (solid), squark (dotted), and Z exchange (dashed). These contributions are calculated from (a) a mSUGRA bino-scenario ($M_1 = \frac{1}{3}\mu$, $M_2 = \frac{2}{3}\mu$), (b) an AMSB wino-scenario ($M_1 = \frac{3}{2}\mu$, $M_2 = \frac{1}{2}\mu$), and (c) a higgsino-scenario ($M_1 = \frac{3}{2}\mu$, $M_2 = 3\mu$). The remaining parameters are $\tan\beta = 4$, squark masses $m_{\tilde{q}} = 2$ TeV, and soft trilinear parameters $A_{\tilde{q}} = 0$, pseudo-scalar Higgs mass $m_A = 500$ GeV, and the nuclear and astrophysical parameters of Table 1.

4 Scattering off Germanium

We now numerically compare the contributions to the scattering rate by the Higgs, squark, and Z exchange in Figures 2. The target sample is germanium to match the CDMS [16] and HDMS [17] collaborations. The nuclear and astrophysical parameters used are listed in Table 1. The nuclear parameters are from the 1988 EMC data [18, 19, 20] and Ref. [21]. For reasonable parameter constraints supplied by AMSB and mSUGRA, we created scenarios with the lightest neutralino as wino-like, bino-like, and higgsino-like. From the numerical results, the Higgs-exchange contribution is seen to be much larger than squark-exchange and Z -exchange, except near the Z propagator's pole.

To analytically demonstrate the Higgs dominance, first consider the effective coupling constant f_q^H of the 4-point interaction that proceeds through Higgs exchange. It is proportional to the MSSM $h\tilde{\chi}\tilde{\chi}$ and $H\tilde{\chi}\tilde{\chi}$ vertices. In the approximations of wino-like lightest neutralino ($\tilde{\chi}_{12}^0 \gg \tilde{\chi}_{11}^0$) and small Higgs mixing angle α , these coupling constants are

$$c_{h\chi\chi} \approx \frac{1}{2}g_2\tilde{\chi}_{12}^0\tilde{\chi}_{14}^0 \quad (20)$$

$$c_{H\chi\chi} \approx -\frac{1}{2}g_2\tilde{\chi}_{12}^0\tilde{\chi}_{13}^0. \quad (21)$$

Further imposing the limits $m_Z/|\mu \pm M_1| \ll 1$, $m_Z/|\mu \pm M_2| \ll 1$, and $\tan\beta > 2$, these coupling constants become [8]

Table 1: Nuclear and astrophysical parameters used for calculations [18, 19, 20, 21].

for protons:		Δu	0.77
f_{Tu}	0.023	Δd	-0.49
f_{Td}	0.034	Δs	-0.15
f_{Ts}	0.14	for ^{73}Ge , $\lambda^2 J(J+1)$	
for neutrons:		F_ξ	1
f_{Tu}	0.019	$v_{\tilde{\chi}}$	320 km/s
f_{Td}	0.041	$\rho_{\tilde{\chi}}$	0.3 GeV/cm ³
f_{Ts}	0.14		

$$c_{h\chi\chi} \approx \frac{g_2}{2} \frac{M_2 + \mu \sin 2\beta}{\mu^2 - M_2^2} m_W \quad (22)$$

$$c_{H\chi\chi} \approx \frac{g_2}{2} \frac{\mu \cos 2\beta}{\mu^2 - M_2^2} m_W. \quad (23)$$

For sketching purposes, these couplings go as $\sim m_W/\mu$. The contribution of Higgs-exchange to the cross section will then go as $\sim m_r^2 m_N^2 / \mu^2 m_h^4$, where m_r is the reduced mass of the nucleon and neutralino.

The coupling, d_q^Z , for $\tilde{\chi}q$ scattering through Z -exchange (Eqn. 19) goes as $\sim m_Z^2/\mu^4$ and contribution to the cross-section goes as $\sim m_r^2 m_Z^4/\mu^8$. The wino- and higgsino-like neutralino scenarios of figures 2(b) and 2(c) show over an order of magnitude Z -exchange increase over the bino-like scenario since their cross-sections are proportional to g_2^4 , versus g_1^4 .

The squark-exchange couplings $f_q^{\tilde{q}}$, $c_q^{\tilde{q}}$, and $d_q^{\tilde{q}}$ are proportional to $a_{\tilde{q}_i}^2 + b_{\tilde{q}_i}^2$, $a_{\tilde{q}_i} b_{\tilde{q}_i}$, and $a_{\tilde{q}_i}^2 - b_{\tilde{q}_i}^2$. $a_{\tilde{q}_i}$ and $b_{\tilde{q}_i}$ will be of the same order for all types of neutralinos if $\tan \beta$ is not extremely large or small. An extreme value of $\tan \beta$ may cause squark-exchange to become more pronounced (see the Appendix for the Z_{q0} coupling). For moderate values of $\tan \beta$, it is because the squark cross-section contribution is proportional to $\sim m_r^2/m_{\tilde{q}}^4$ that squark exchange is suppressed when a heavy squark is considered.

Fig. 3 shows the numerically calculated scattering rates for neutralinos and ^{73}Ge at $\tan \beta = 4$ for the three cases of “moderate” values of the squark mass ($m_{\tilde{q}} = 2$ TeV) and pseudo-scalar Higgs masses ($m_A = 500$ GeV), a light squark ($m_{\tilde{q}} = 500$ GeV) case, and a light pseudo-scalar Higgs ($m_A = 150$ GeV) case. The practical aspect of these plots lies in recognizing the various possibilities of tuning the cross-section and scattering rate by varying the supersymmetry breaking model parameters μ , $m_{\tilde{q}_i}$, and m_A along with $\tan \beta$. The rates for ^{76}Ge are similar to those for ^{73}Ge since the spin-dependent contributions are small for

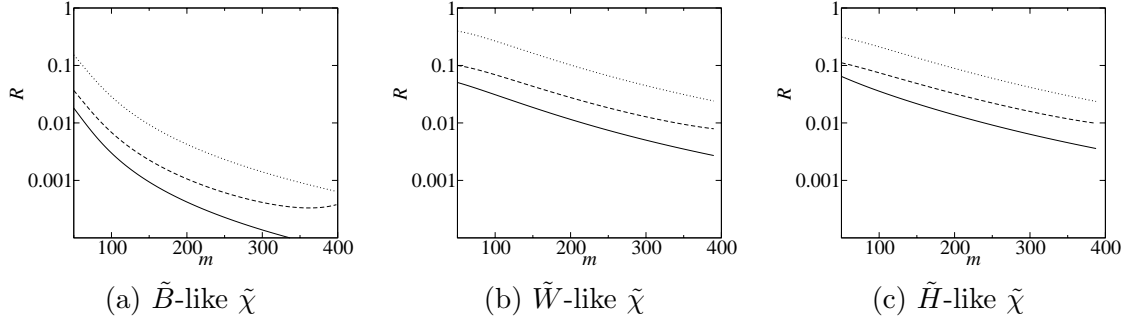


Figure 3: The $\tilde{\chi}$ - ^{73}Ge scattering rates R (events/day/kg) as a function of the LSP mass $m_{\tilde{\chi}}$ (GeV) for bino, wino, and higgsino scenarios. Scenario (a) uses $M_1 = \frac{1}{3}\mu$, $M_2 = \frac{2}{3}\mu$, (b) uses $M_1 = \frac{3}{2}\mu$, $M_2 = \frac{1}{2}\mu$, and (c) uses $M_1 = \frac{3}{2}\mu$, $M_2 = 3\mu$. The solid lines have “moderate” parameters $m_{\tilde{q}} = 2$ TeV, $m_A = 500$ GeV. The dashed lines represent a light squark with $m_{\tilde{q}} = 500$ GeV, $m_A = 500$ GeV. The dotted lines represent a light pseudo-scalar Higgs with $m_{\tilde{q}} = 2$ TeV, $m_A = 150$ GeV. For all, $\tan\beta = 4$ and soft trilinear parameters $A_{\tilde{q}} = 0$ are used.

both.

The bino-like neutralino scattering rate suffers from the lower g_1 coupling constant, explicit in Eqs. 24 and 25. The wino- and higgsino-like neutralinos have comparable scattering rates due to the common vertices that originate from the Lagrangian terms $-\frac{1}{\sqrt{2}}g_2 H_i \tilde{H}_i \tilde{W}^3$. The bino-like neutralino has analogous terms but are proportional to the smaller U(1) gauge coupling g_1 .

While these calculations show promising event rates for a wide range of parameter space, the regions of parameter space that result in undetectable scattering rates should be noted. Larger values of $\tan\beta$ will lower the $h\bar{t}t$ coupling (Eq. 28) and suppress the light Higgs exchange. Large $\tan\beta$ also slightly increases the light Higgs mass m_h and causes further suppression. In the case of light squarks, a large $\tan\beta$ has the opposite effect — enhancing the scattering rate by causing significant left-right squark mixing, driving the sbottom and stop masses down. The corresponding squark propagators are then enhanced. Overriding the effects of varying $\tan\beta$, larger mass parameters for the Higgs, gauginos, and squarks can quickly reduce the scattering rate to undetectable levels. When $\tan\beta \gg 1$ the cross-section begins to rise again. One can show that the cross-section starts to rise like $\tan^2\beta$ when $\tan\beta \gtrsim m_H^2/m_h^2$ due to the increased relative importance of the heavier Higgs boson.

5 DAMA Constraints on Supersymmetry Parameters

The DAMA collaboration reports [22] indications of a WIMP with a mass of 52_{-8}^{+10} GeV and a cross-section of $\xi\sigma_{\text{scalar}} = 7.2_{-0.9}^{+0.4} \times 10^{-6}$ pb when scattered against a single proton, using

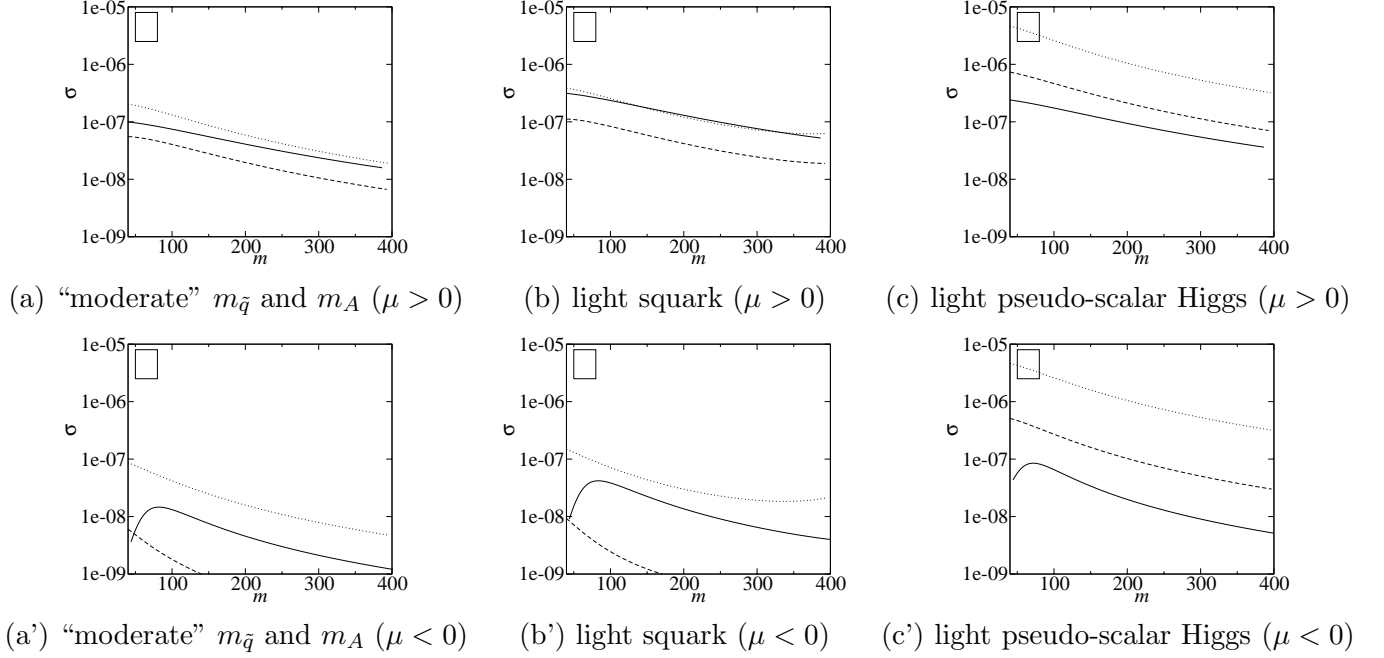


Figure 4: Illustrations of the DAMA constraints (roughly equivalent to the boxes in each figure panel). Each plot represents the scalar (spin-independent) contribution to the cross-section σ_{scalar} (pb) as a function of the wino-like neutralino mass $m_{\tilde{\chi}}$ (GeV) for neutralino-proton scattering in an AMSB scenario ($M_1 = \frac{3}{2}\mu$, $M_2 = \frac{1}{2}\mu$). (a) represents “moderate” parameters ($m_{\tilde{q}} = 2$ TeV, $m_A = 500$ GeV), (b) represents a light squark scenario ($m_{\tilde{q}} = 500$ GeV, $m_A = 500$ GeV), and (c) represents a light pseudo-scalar Higgs scenario ($m_{\tilde{q}} = 2$ TeV, $m_A = 200$ GeV). $A_{\tilde{q}} = 0$ is used for all soft trilinear parameters. The values of $\tan \beta$ are 2 (solid), 10 (dashed) and 30 (dotted). The upper (lower) set of plots have values $\mu > 0$ ($\mu < 0$).

standard astrophysical assumptions (as in Table 1). ξ is the fraction of the cold dark matter that this WIMP represents. The “scalar” subscript on the cross-section refers to only the spin-independent contributions.

We apply our analysis to interpret this WIMP signal as a scattering of the lightest neutralino. The AMSB wino scenario is chosen as the framework for this interpretation without too much loss of generality. One can roughly equate this with the higgsino scenario, or take off an order of magnitude from the scattering rate to imagine the mSUGRA bino scenario (as in Fig. 3).

We have made assumptions about the astrophysical and squark parameters ($A_{\tilde{q}}$ and $m_{\tilde{q}}$). Altering the astrophysical models, i.e. the galactic halo structure, may significantly change the allowed SUSY parameter space. Refs. [23, 24, 25] demonstrate a means for different galactic halo models to allow for WIMP masses up to 150 GeV at 3σ . Non-universal squark masses and soft trilinear parameters allow for a broad range of cross-sections for any fixed set of values $m_{\tilde{\chi}}$, $\tan\beta$, and $\text{sgn}(\mu)$, as seen in Refs. [26, 27, 28, 29]. As for assumptions on the nuclear parameters, Ref. [30] demonstrates the effect of uncertainties of the quark masses and mass fractions f_{Tq} .

Using the “moderate” SUSY parameters of Fig. 4(a) ($m_{\tilde{q}} = 2$ TeV, $m_A = 500$ GeV, $A_{\tilde{q}} = 0$) the cross section is significantly below the favored region of the DAMA/NaI-2 data. The lighter squark of Fig. 4(b) will increase the scalar cross-section, but not to DAMA heights. A light pseudo-scalar Higgs is necessary for compatibility with the DAMA limits. By tuning $\tan\beta$, $m_{\tilde{q}}$, and m_A the DAMA interpretation may be made compatible with anomaly and gravity mediated SUSY breaking models.

One concern with the above parameter space with light pseudo-scalar is that the lightest CP-even Higgs mass will fall below the LEP-II limits. Indeed, our lightest Higgs mass in our examples range from about 100 GeV to 115 GeV which is just at the LEP-II SM Higgs limits. However, one should keep in mind that the LEP-II SUSY Higgs limits are significantly below the SM Higgs limits due to decreased hZZ coupling when the pseudo-scalar is light. Furthermore, our result for matching the DAMA allowed region is mostly independent of the light Higgs mass or the squark masses. Therefore, the rest of the superpartner masses can arrange themselves to produce large enough loop corrections to satisfy the Higgs mass constraints without significantly affecting our final result.

6 Conclusions

We complement previous efforts to demonstrate the compatibility of supersymmetry and the recent DAMA annual modulation signal [27]-[35] by showing that the wino-like LSP from AMSB models are also compatible with the DAMA signal. Furthermore, the AMSB models lead to detectable event rates for a large volume of SUSY parameter space through the tuning of $\tan\beta$, $m_{\tilde{q}}$, and m_A . The AMSB-inspired models produce nearly identical event rates if a higgsino is the LSP. This is due to the dominance of Higgs exchange and the $\tilde{H}_i \leftrightarrow \tilde{W}$ symmetry in the $-\frac{1}{\sqrt{2}}g_2 H_i \tilde{H}_i \tilde{W}^3$ operators.

mSUGRA and AMSB models differ by about an order of magnitude in the event rate when mSUGRA produces a bino-like LSP, due mainly to the differences of the SU(2) and U(1) gauge couplings. The wino-like neutralino's event rate is always higher than the bino-like neutralino's for all of parameter space.

Although the WIMP mass and cross-section implied by DAMA's recent observations are confirmed to be compatible with mSUGRA and AMSB models, the necessary parameters are near the edge of what is ruled out by other experiments, such as collider physics. For wino and higgsino LSPs, the masses can be rather light (certainly lower than 80 GeV) without running into collider constraints because it is so difficult to find winos and higgsinos at colliders [36]-[39].

Appendix: MSSM Coupling Constants

For the Higgs-fermion-fermion vertices, using the notation of Drees and Nojiri (Ref [13]):

$$c_{h\tilde{\chi}\tilde{\chi}} = \frac{1}{2}(g_2 N_{12} - g_1 N_{11})(\sin\alpha N_{13} + \cos\alpha N_{14}) \quad (24)$$

$$c_{H\tilde{\chi}\tilde{\chi}} = \frac{1}{2}(g_2 N_{12} - g_1 N_{11})(-\cos\alpha N_{13} + \sin\alpha N_{14}) \quad (25)$$

$$c_{hdd} = \frac{g_2}{2m_W} \frac{\sin\alpha}{\cos\beta} \quad (26)$$

$$c_{Hdd} = -\frac{g_2}{2m_W} \frac{\cos\alpha}{\cos\beta} \quad (27)$$

$$c_{huu} = -\frac{g_2}{2m_W} \frac{\cos\alpha}{\sin\beta} \quad (28)$$

$$c_{Huu} = -\frac{g_2}{2m_W} \frac{\sin\alpha}{\sin\beta} \quad (29)$$

where α is the Higgs mixing angle.

For the $Z\tilde{\chi}\tilde{\chi}$ vertex:

$$O_R'' = \frac{1}{2} [|N_{14}|^2 - |N_{13}|^2] \quad (30)$$

For the $\tilde{q}q\tilde{\chi}$ vertices:

$$a_{\tilde{q}_1} = \frac{1}{2} [\cos \theta_{\tilde{q}} (X_{q0} + Z_{q0}) + \sin \theta_{\tilde{q}} (Y_{q0} + Z_{q0})] \quad (31)$$

$$a_{\tilde{q}_2} = \frac{1}{2} [-\sin \theta_{\tilde{q}} (X_{q0} + Z_{q0}) + \cos \theta_{\tilde{q}} (Y_{q0} + Z_{q0})] \quad (32)$$

$$b_{\tilde{q}_1} = \frac{1}{2} [\cos \theta_{\tilde{q}} (X_{q0} - Z_{q0}) + \sin \theta_{\tilde{q}} (-Y_{q0} + Z_{q0})] \quad (33)$$

$$b_{\tilde{q}_2} = \frac{1}{2} [-\sin \theta_{\tilde{q}} (X_{q0} - Z_{q0}) + \cos \theta_{\tilde{q}} (-Y_{q0} + Z_{q0})] \quad (34)$$

where $\theta_{\tilde{q}}$ is the squark mixing angle of left and right squarks into physical squarks and

$$X_{q0} = -\sqrt{2}g_2[T_{q3}N_{12} - \tan \theta_W(T_{q3} - e_q)N_{11}] \quad (35)$$

$$Y_{q0} = \sqrt{2}g_2 \tan \theta_W e_q N_{11} \quad (36)$$

$$Z_{q0} = \begin{cases} -\frac{g_2 m_u N_{14}}{\sqrt{2} \sin \beta m_W} & \text{for up-type quarks} \\ -\frac{g_2 m_d N_{13}}{\sqrt{2} \cos \beta m_W} & \text{for down-type quarks.} \end{cases} \quad (37)$$

References

- [1] J. Ellis, J. S. Hagelin, D. V. Nanopoulos, K. Olive and M. Srednicki, “Supersymmetric relics from the big bang,” Nucl. Phys. **B238**, 453 (1984).
- [2] For example, see E. Diehl, G. L. Kane, C. Kolda and J. D. Wells, “Theory, phenomenology, and prospects for detection of supersymmetric dark matter,” Phys. Rev. **D52**, 4223 (1995) [hep-ph/9502399].
- [3] S. Mizuta, D. Ng and M. Yamaguchi, “Phenomenological aspects of supersymmetric standard models without grand unification,” Phys. Lett. **B300**, 96 (1993) [hep-ph/9210241].
- [4] L. Randall and R. Sundrum, “Out of this world supersymmetry breaking,” Nucl. Phys. **B557**, 79 (1999) [hep-th/9810155].
- [5] G. F. Giudice, M. A. Luty, H. Murayama and R. Rattazzi, “Gaugino mass without singlets,” JHEP **9812**, 027 (1998) [hep-ph/9810442].
- [6] J. A. Bagger, T. Moroi and E. Poppitz, “Anomaly mediation in supergravity theories,” JHEP **0004**, 009 (2000) [hep-th/9911029].

- [7] T. Gherghetta, G. F. Giudice and J. D. Wells, “Phenomenological consequences of supersymmetry with anomaly-induced masses,” Nucl. Phys. **B559**, 27 (1999) [hep-ph/9904378].
- [8] T. Moroi and L. Randall, “Wino cold dark matter from anomaly-mediated SUSY breaking,” Nucl. Phys. **B570**, 455 (2000) [hep-ph/9906527].
- [9] A. Brignole, L. E. Ibanez and C. Munoz, “Towards a theory of soft terms for the supersymmetric Standard Model,” Nucl. Phys. **B422**, 125 (1994) [hep-ph/9308271].
- [10] J. Amundson, *et al.*, “Report of the Supersymmetry Theory Subgroup,” hep-ph/9609374.
- [11] G. Jungman, M. Kamionkowski and K. Griest, “Supersymmetric dark matter,” Phys. Rept. **267**, 195 (1996) [hep-ph/9506380].
- [12] H. E. Haber and G. L. Kane, “The Search For Supersymmetry: Probing Physics Beyond The Standard Model,” Phys. Rept. **117**, 75 (1985).
- [13] M. Drees and M. Nojiri, “Neutralino - nucleon scattering revisited,” Phys. Rev. **D48**, 3483 (1993) [hep-ph/9307208].
- [14] M. Drees and M. M. Nojiri, “New contributions to coherent neutralino - nucleus scattering,” Phys. Rev. **D47**, 4226 (1993) [hep-ph/9210272].
- [15] J. Ellis and M. Karliner, “Analysis of data on polarized lepton - nucleon scattering,” Phys. Lett. **B313**, 131 (1993) [hep-ph/9305306].
- [16] R. Abusaidi *et al.* [CDMS Collaboration], “Exclusion limits on the WIMP nucleon cross-section from the Cryogenic Dark Matter Search,” Nucl. Instrum. Meth. **A444**, 345 (2000) [astro-ph/0002471].
- [17] L. Baudis, A. Dietz, B. Majorovits, F. Schwamm, H. Strecker and H. V. Klapdor-Kleingrothaus, “First results from the Heidelberg dark matter search experiment,” astro-ph/0008339.
- [18] J. Ashman *et al.* [European Muon Collaboration], “An investigation of the spin structure of the proton in deep inelastic scattering of polarized muons on polarized protons,” Nucl. Phys. **B328**, 1 (1989).
- [19] H. Cheng, “Low-Energy Interactions Of Scalar And Pseudoscalar Higgs Bosons With Baryons,” Phys. Lett. **B219**, 347 (1989).

- [20] R. L. Jaffe and A. Manohar, “The G(1) Problem: Fact And Fantasy On The Spin Of The Proton,” Nucl. Phys. **B337**, 509 (1990).
- [21] J. Ellis and R. A. Flores, “Elastic supersymmetric relic - nucleus scattering revisited,” Phys. Lett. **B263**, 259 (1991).
- [22] R. Bernabei *et al.* [DAMA Collaboration], “Search for WIMP annual modulation signature: Results from DAMA / NaI-3 and DAMA / NaI-4 and the global combined analysis,” Phys. Lett. **B480**, 23 (2000).
- [23] M. Kamionkowski and A. Kinkhabwala, “Galactic halo models and particle dark matter detection,” Phys. Rev. **D57**, 3256 (1998) [hep-ph/9710337].
- [24] M. Brhlik and L. Roszkowski, “WIMP velocity impact on direct dark matter searches,” Phys. Lett. **B464**, 303 (1999) [hep-ph/9903468].
- [25] A. M. Green, “The WIMP annual modulation signal and non-standard halo models,” astro-ph/0008318.
- [26] J. Berezhinsky, *et al.*, “Neutralino dark matter in supersymmetric models with nonuniversal scalar mass terms,” Astropart. Phys. **5**, 1 (1996) [hep-ph/9508249].
- [27] J. Ellis, A. Ferstl and K. A. Olive, “Exploration of elastic scattering rates for supersymmetric dark matter,” hep-ph/0007113.
- [28] A. Corsetti and P. Nath, “SUSY dark matter,” hep-ph/0005234.
- [29] E. Accomando, R. Arnowitt, B. Dutta and Y. Santoso, “Neutralino proton cross sections in supergravity models,” Nucl. Phys. **B585**, 124 (2000) [hep-ph/0001019].
- [30] A. Bottino, F. Donato, N. Fornengo and S. Scopel, “Implications for relic neutralinos of the theoretical uncertainties in the neutralino nucleon cross-section,” Astropart. Phys. **13**, 215 (2000) [hep-ph/9909228].
- [31] A. B. Lahanas, D. V. Nanopoulos and V. C. Spanos, “Neutralino dark matter elastic scattering in a flat and accelerating universe,” hep-ph/0009065.
- [32] R. Arnowitt and P. Nath, “Annual modulation signature for the direct detection of Milky Way wimps and supergravity models,” Phys. Rev. **D60**, 044002 (1999) [hep-ph/9902237].
- [33] R. Arnowitt, B. Dutta and Y. Santoso, “Maximum and minimum dark matter detection cross sections,” hep-ph/0008336.

- [34] V. Mandic, A. Pierce, P. Gondolo and H. Murayama, “The lower bound on the neutralino nucleon cross section,” hep-ph/0008022.
- [35] A. Bottino, F. Donato, N. Fornengo and S. Scopel, “Further investigation of a relic neutralino as a possible origin of an annual-modulation effect in WIMP direct search,” Phys. Rev. **D62**, 056006 (2000) [hep-ph/0001309].
- [36] C. H. Chen, M. Drees and J. F. Gunion, “Searching for Invisible and Almost Invisible Particles at e^+e^- Colliders,” Phys. Rev. Lett. **76**, 2002 (1996) [hep-ph/9512230].
- [37] S. Thomas and J. D. Wells, “Massive doublet leptons,” Phys. Rev. Lett. **81**, 34 (1998) [hep-ph/9804359].
- [38] J. L. Feng, T. Moroi, L. Randall, M. Strassler and S. Su, “Discovering supersymmetry at the Tevatron in Wino LSP scenarios,” Phys. Rev. Lett. **83**, 1731 (1999) [hep-ph/9904250].
- [39] J. F. Gunion and S. Mrenna, “A study of SUSY signatures at the Tevatron in models with near mass degeneracy of the lightest chargino and neutralino,” Phys. Rev. **D62**, 015002 (2000) [hep-ph/9906270].